## Werk

**Jahr:** 1980
**Kollektion:** fid.geo
**Signatur:** 8 Z NAT 2148:48
**Digitalisiert:** Niedersächsische Staats- und Universitätsbibliothek Göttingen
**Werk Id:** PPN1015067948_0048
**PURL:** http://resolver.sub.uni-goettingen.de/purl?PPN1015067948_0048

**LOG Id:** LOG_0018
**LOG Titel:** Maximum velocity amplitudes of P and S waves from filtered broadband records
**LOG Typ:** article

## Übergeordnetes Werk

**Werk Id:** PPN1015067948
**PURL:** http://resolver.sub.uni-goettingen.de/purl?PPN1015067948
**OPAC:** http://opac.sub.uni-goettingen.de/DB=1/PPN?PPN=1015067948



## Contact

Niedersächsische Staats- und Universitätsbibliothek Göttingen
Georg-August-Universität Göttingen
Platz der Göttinger Sieben 1
37073 Göttingen
Germany
Email: gdz@sub.uni-goettingen.de

J Geophys. 48, 47–53, 1980

Journal of Geophysics

# Maximum Velocity Amplitudes of *P* and *S* Waves From Filtered Broadband Records

M.V.D. Sitaram[1], A. Plešinger[2], and J. Vaněk[2]

[1] National Geophysical Research Institute, Hyderabad, 500007, India
[2] Geophysical Institute, Czechoslovak Academy of Sciences, 14131 Praha 4, Czechoslovakia

**Abstract.** The maximum velocity amplitudes ($A_{vmax}$) of *P* and *S* waves in different period bands are studied using filtered broadband records from the KHC Seismic Station. Two sequences of shallow earthquakes from the Tadzhik-Sinkiang border and from North-eastern China with magnitudes $m_b$ between 5.0 and 6.3 are investigated. Amplitude-periodband (APB) diagrams are constructed for each event. The largest values of $A_{vmax}$ are found in the period band from 2.2 to 10 s for *P* waves and from 3.4 to 23 s for *S* waves. A shift of the maximum in the APB diagrams towards longer periods for earthquakes with $m_b > 6.0$ is observed. For events with $m_b < 6.0$ the position of the maximum virtually does not depend on the magnitude. This phenomenon seems to be related with the process of wave generation in the focal region.

**Key words:** Seismology – Earthquake magnitude – Maximum velocity amplitudes – Broadband records.

## Introduction

A more profound knowledge of the physical principles of the earthquake magnitude seems to be one of the substantial conditions for an improvement of routine magnitude determinations. Especially, a comprehensive investigation into the properties of the observational basis of the magnitude, the maximum ratio of amplitude and period $(A/T)_{max}$ for the individual wave types, is very desirable. In this context the behaviour of the quantity $(A/T)_{max}$ in different period ranges appears to be essential. Several papers reporting on results of investigations in this direction have been published (Korchagina and Moskvina 1972; Zapolskij et al. 1974; Aranovich et al. 1977; Roglinov et al. 1978).

The aim of the present study is to analyze the maximum velocity amplitudes of *P* and *S* waves in the period range from 1 to 170 s on the basis of a sequence of filtered broadband records for two series of shallow earthquakes.

## 1 Observational Material and Method of Data Processing

For the present study two sequences of shallow earthquakes from the Tadzhik-Sinkiang border (TSB) and from North-eastern China (NEC) were used. The parameters of the individual earthquakes are listed in Table 1. The respective observational material was obtained from the magnetic tape library of the FBV Broadband Seismograph System operating at the KHC Seismic Station (Kašperské Hory in South Bohemia, $\varphi = 49°07.8'$N, $\lambda = 13°34.8'$E). The variation of the epicentral co-ordinates is so small that the wave propagation paths to KHC are nearly the same for all events in each series. The epicentral distances for the TSB and NEC events are, respectively, about 43° and 69.5°

The FBV system has a flat-velocity response in the period range $0.3 < T < 300$ s. Each component (Z, NS, EW) is recorded bi-level in an overall dynamic range of 80 dbs on 12-track FM magnetic tape. For the processing of the tapes the DPS Data Processing System containing proper analogue and hybrid devices is used in the Geophysical Institute at Prague. Both systems are described in a previous paper by Plešinger and Horálek (1976).

To obtain the data in the form needed for the present study the FBV records were processed in the following way. The vertical and the horizontal components of each event were passed through a set of twelve one-octave 4th-degree Butterworth filters. The passbands of the individual filters and their centre periods are given in Table 2. The centre periods cover the range from 1.5 to 128 s in half-octave steps. Simultaneously, a procedure of particle motion analysis that discriminates *P*, *S*, and *LR* waves was performed. The outputs of the individual filters and the output of the particle motion analyzer were recorded by a linear multichannel high-speed heat-pen recorder (see Fig. 1). On each of the filtered records three quantities of the *P* and *S* wave groups were measured for every component: the maximum amplitude from trough to peak or vice versa, the period corresponding to the maximum amplitude, and the time difference between the first onset of the wave group and the occurrence of the maximum amplitude. In the majority of cases the signal-to-noise ratio was high enough to enable an undistorted evaluation. It became necessary, however, to employ also few wave groups with amplitudes comparable with those of the noise in the respective period band in order to find out the general trends and the maxima of the curves investigated in Sect. 2.

Since the FBV system has a broadband flat-velocity response the maximum amplitudes determined in the way outlined above, converted into ground velocity and divided by $2\pi$, directly give the value of $(A/T)_{max}$ which is the basic parameter for magnitude estimations.

## 2. Amplitude-Periodband Diagrams

For the graphical representation of the dependence of the maximum velocity amplitudes on the filter passbands we use the term 'amplitude-periodband diagrams' in this paper and denote them briefly APB diagrams. These diagrams are analogous to the so-called 'velocity spectra' introduced by Bune et al. (1973) and Za-

0340-062X/80/0048/0047/$01.40

**Table 1.** Parameters of earthquakes

| Event | Date | | Origin time | Latitude | Longitude | Depth (km) | $m_b$ | Source |
|---|---|---|---|---|---|---|---|---|
| TSB 1 | 1974 August | 11 | 01:13:55 | 39.34N | 73.76E | 7 | 6.2 | ISC |
| 2 | | 11 | 05:12:35.1 | 39.33N | 73.75E | 48 | 5.3 | |
| 3 | | 11 | 05:23:57.3 | 39.32N | 73.75E | 72 | 5.4 | |
| 4 | | 11 | 07:02:07 | 39.34N | 73.80E | 18 | 5.1 | |
| 5 | | 11 | 20:05:30.9 | 39.44N | 73.67E | 41 | 5.7 | |
| 6 | | 11 | 21:21:37.1 | 39.46N | 73.62E | 26 | 5.8 | |
| 7 | | 27 | 12:56:01.0 | 39.52N | 73.82E | 19 | 5.7 | |
| 8 | | 27 | 17:33:58.6 | 39.34N | 73.86E | 37 | 5.1 | |
| 9 | 1974 September | 03 | 19:41:21.1 | 39.42N | 73.74E | 43 | 5.3 | |
| NEC 1 | 1976 July | 27 | 19:42:54.6 | 39.57N | 117.98E | 22.8 | 6.3 | NEIS |
| 2 | | 27 | 23:17:31.4 | 39.36N | 117.82E | 31.4 | 5.4 | |
| 3 | | 28 | 00:58:46.9 | 39.41N | 117.78E | 33.0 | 5.0 | |
| 4 | | 28 | 10:45:35.2 | 39.66N | 118.40E | 26.4 | 6.3 | |
| 5 | | 28 | 15:35:55.3 | 39.85N | 118.66E | 13.0 | 5.3 | |
| 6 | | 29 | 01:01:03.2 | 39.92N | 118.88E | 35.4 | 5.1 | |
| 7 | | 30 | 21:23:15.0 | 39.82N | 118.33E | 33.0 | 5.4 | |
| 8 | 1976 August | 31 | 03:25:27.8 | 39.80N | 118.86E | 31.8 | 5.3 | |
| 9 | 1976 November | 15 | 13:53:00.6 | 39.44N | 117.69E | 15.2 | 6.0 | |

**Table 2.** System of filters

| Number of filter | Passband (seconds) | Centre period (seconds) |
|---|---|---|
| I | 1.0– 2.0 | 1.5 |
| II | 1.5– 3.0 | 2.2 |
| III | 2.2– 4.5 | 3.4 |
| IV | 3.4– 6.8 | 5.1 |
| V | 5.0– 10.0 | 7.5 |
| VI | 7.5– 11.0 | 11.0 |
| VII | 11.5– 23.0 | 17.0 |
| VIII | 17.0– 34.0 | 25.0 |
| IX | 25.0– 50.0 | 35.0 |
| X | 37.0– 75.0 | 56.0 |
| XI | 56.0–112.0 | 84.0 |
| XII | 85.0–170.0 | 128.0 |

polskij et al. (1974) on the basis of observations with Frequency Selecting Seismic Stations (ČISS). It must be noticed, however, that APB diagrams cannot be considered to be identical with velocity amplitude spectra because they express the dependence of two quite different quantities (maximum amplitude instead of the root of spectral density, filter passband instead of frequency). In general, no prominent similarity must exist between APB diagrams and amplitude spectra of *P* and *S* waves for teleseismic events. A special study of the relation between APB diagrams and amplitude spectra is underway and the results will be published in a separate paper.

In the present study, the APB diagrams were constructed for the vertical and horizontal components (*Z*, *NS*, and *EW*) of *P* and *S* waves for both the TSB and NEC events. To illustrate the reliability of the results two typical APB diagrams of the seismic noise level at KHC are shown in Fig. 2.

### *2.1. APB Diagrams for P Waves*

The resulting APB diagrams for *P* waves are shown in Fig. 3, maximum velocity amplitudes in microns per second being plotted in the logarithmic scale. Number of event and the corresponding magnitude $m_b$ are indicated for every curve. The solid circles indicate values of $A_{vmax}$ which were safely above the noise level. Values of $A_{vmax}$ evaluated from readings with comparable signal and noise amplitudes are denoted by open circles. Some of these cases were included in order to find out the trends of the APB curves, especially in their long-period flanks.

The general shape of the APB diagrams for all three components of *P* waves obviously is similar for both the TSB and NEC regions. The diagrams usually have a single pronounced maximum in the range of periods represented by filters III, IV, and V. An exception is the NS component for event No. 1 from the TSB region. For events with larger magnitudes the maxima tend to shift towards longer periods. The levels of the curves correspond to the order of magnitude $m_b$ with the exception of NEC event No. 7 for which $m_b = 5.4$ given by NEIS seems to be too large in comparison with our observations. The anomalous level of the curve for the NS component of NEC event No. 5 is probably due to the disturbing effect of noise in the period band of filters III and IV.

The decrease of maximum velocity amplitudes for passbands in the short-period range is more expresssive for the *Z* and *EW* components of events from the NEC region than for those from the TSB region.

### *2.2. APB Diagrams for S Waves*

The APB diagrams for *S* waves are shown in Fig. 4. In general, they have a similar character as those for *P* waves but the maxima of curves occur at longer periods, i.e., in the range of filters IV to VII for the TSB events and V to IX for the NEC events.

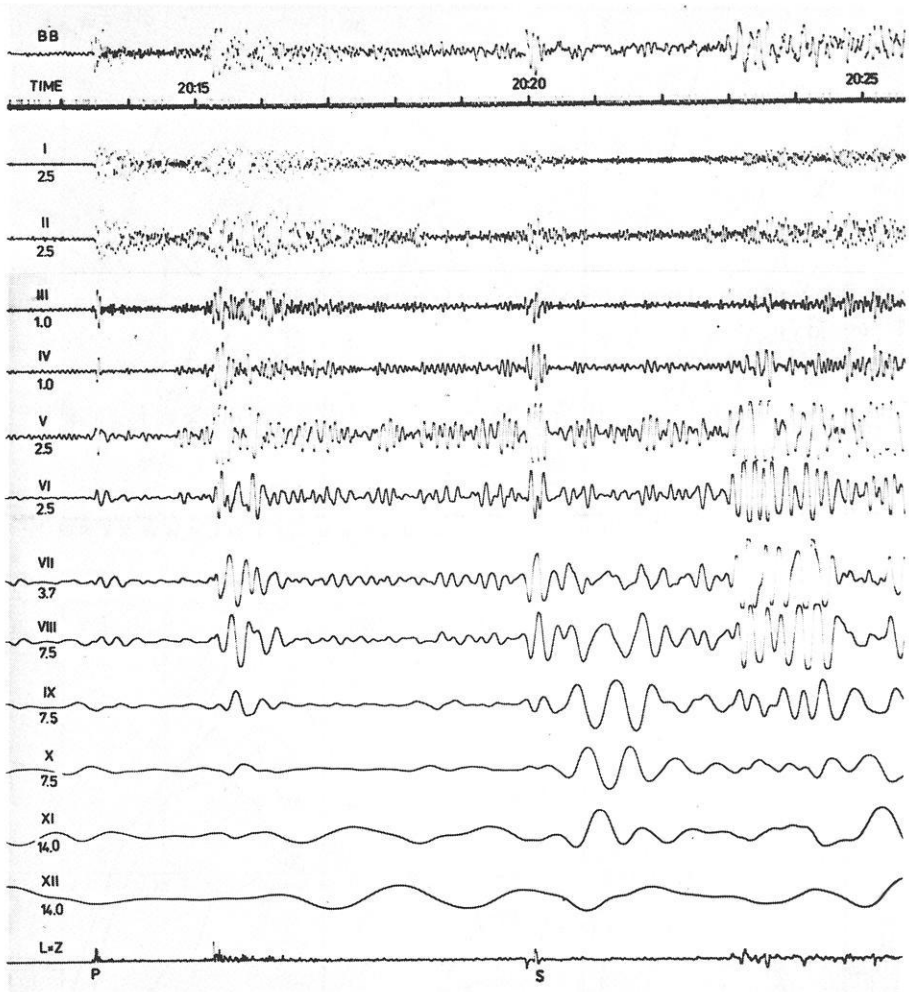


**Fig. 1.** Example of filtered broadband records (event TSB 5, component EW). Trace 1: broadband signal (0.3 to 300 s), trace 2: coded time, traces 3 to 14: outputs of filters I to XII (the arabic numbers are the relative amplification coefficients of the individual channels), trace 15: result of polarization analysis (product of longitudinal and vertical broadband components)

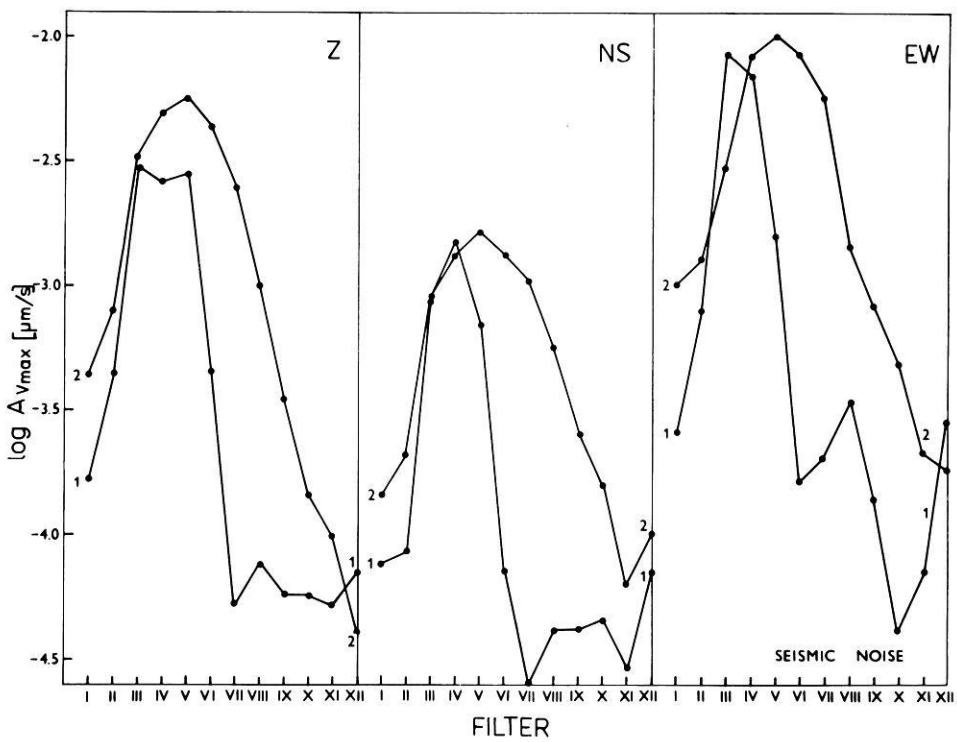


**Fig. 2.** APB diagrams of the seismic noise preceding events TSB 4 (1) and NEC 3 (2). $A_{vmax}$ are the maximum values observed in a time interval of 3 min before the onset of the *P* wave

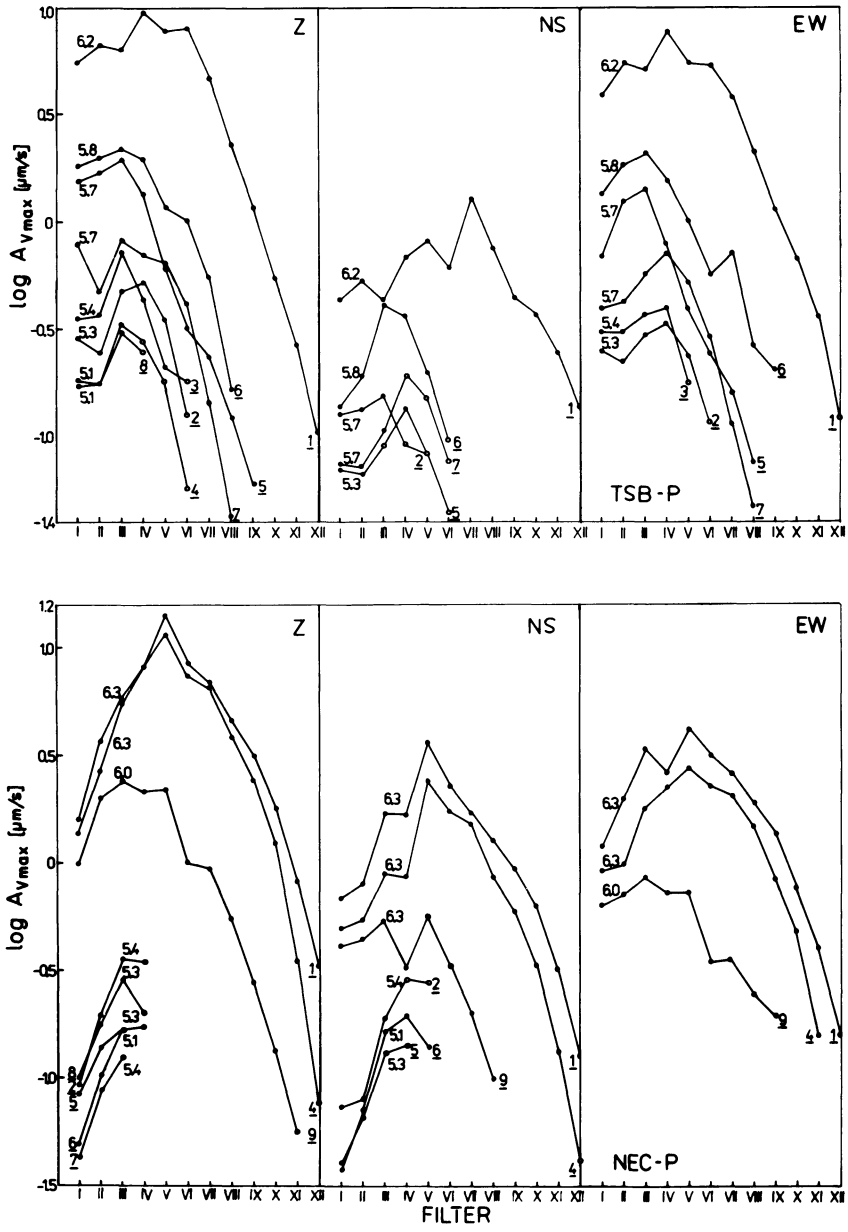


**Fig. 3.** Amplitude-periodband diagrams of *P* waves from the TSB (Tadzhik-Sinkiang border) and NEC (North-eastern China) events. $A_{vmax}$ values above the noise level are denoted by *solid points*, those comparable with the noise level by *circles*. The underlined numbers correspond to the event numbers in Table 1. The decimal numbers are the $m_b$ magnitudes of the individual events (the correct $m_b$ for diagram 9 in figure NEC-P, component NS, is 6.0)

In comparison with *P* waves the maxima of the diagrams are not so well pronounced for most of the events. The $A_{vmax}$ values are comparable in more passbands so that the maximum cannot be unambiguously attached to an individual filter (see, e.g., TSB event No. 6 and NEC events Nos. 1 and 4 in the NS component or TSB event No. 1 in the *EW* component).

The shape of the APB diagrams is also influenced by the internal structure of the wave group investigated. For instance, a detailed polarization analysis of the *S* wave group of TSB event No. 1 has revealed that this group consisted of a pure SH pulse with a half-period of approximately 12 s and a slightly later wave group of rather SV type with a predominant period of about 36 s. This means that $A_{vmax}$ in different passbands can correspond to different wave types.

A tendency of shifting of the maxima of the APB curves towards longer periods for events with larger magnitudes is again observed also for *S* waves.

### *2.3. Time of Occurrence of Maximum Velocity Amplitude*

In our study the problem of the time of occurrence $\tau$ of maximum velocity amplitude in the *P* and *S* wave groups for different filters has been also investigated. Knowledge of $\tau$ values to be expected in different passbands is important for the routine determination of earthquake magnitudes on the basis of maximum amplitudes. The quantity $\tau$ was measured from the onsets of the *P* and *S* wave group. The values for *P* waves were determined from the vertical components, those for *S* waves from the *EW* components of the filtered broadband records. The behaviour of $\tau$ for a set of selected events is shown in Fig. 5.

It is evident that $\tau$ increases with increasing centre periods of the filters as well as with increasing magnitude of the events. Its variation appears to be negligible up to the period range of filter VII. In the passband from 1 s up to approximately 20 s the time of occurrence of the maximum velocity amplitude usually

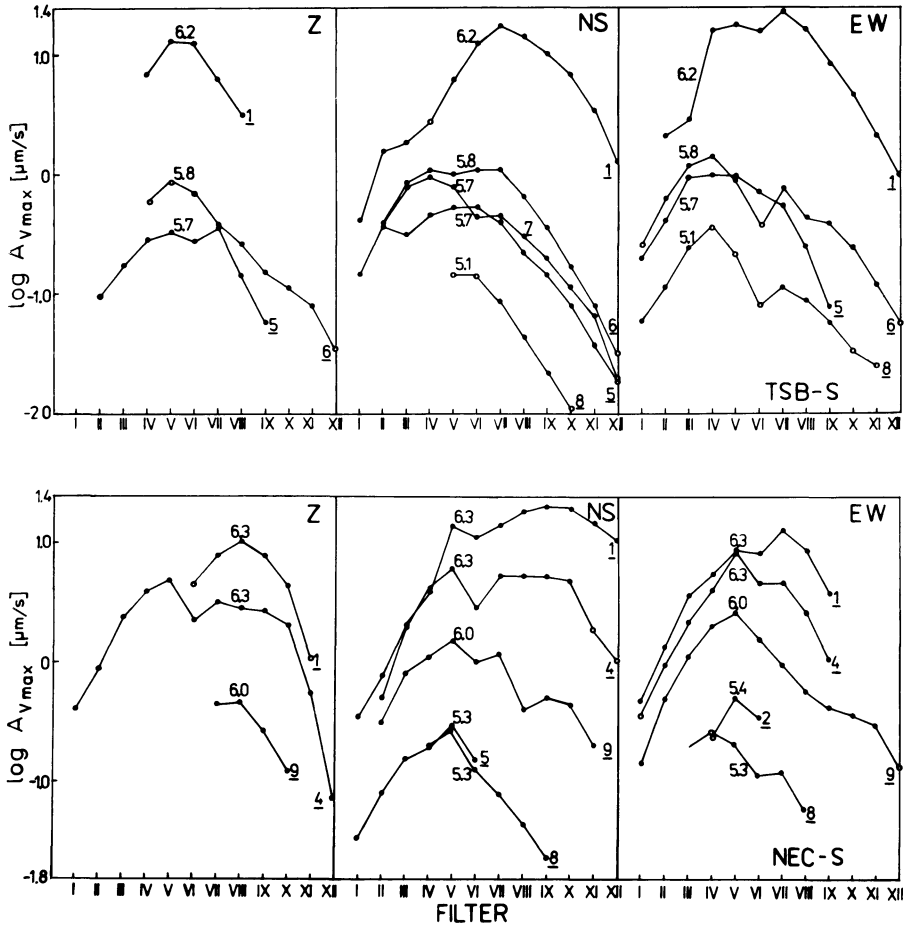


**Fig. 4.** Amplitude-periodband diagrams of $S$ waves from the TSB and NEC events. The individual values and curves are denoted in the same manner as in Fig. 1

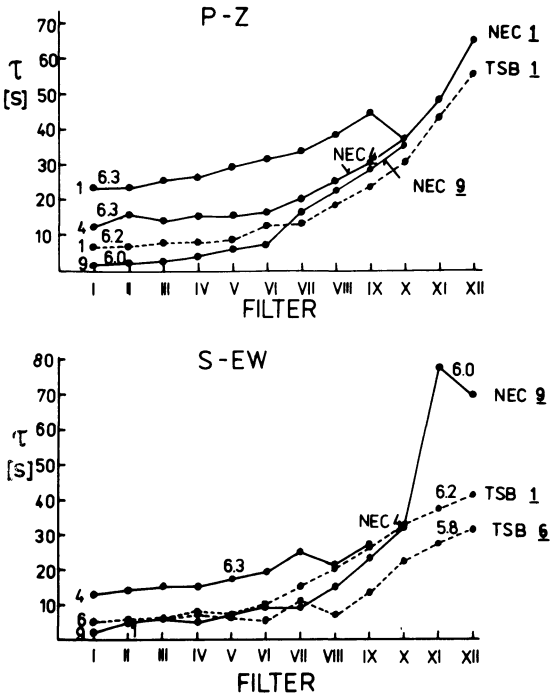


**Fig. 5.** Time of occurrence $\tau$ of maximum velocity amplitude vs. period-passband (filter number) for a set of selected events

does not exceed 30 s for both $P$ and $S$ waves. The variation of $\tau$ in the long-period range is considerable, reaching up to 80 s for $S$ as well as $P$ waves.

## 3. Discussion

A comparison of the APB diagrams in Figs. 3 and 4 indicates that there exists a stable relation between the three components of $P$ and $S$ waves for any of the events investigated. It should, therefore, be sufficient to select only one component for investigations of this kind. For $P$ waves the vertical component and for $S$ waves one of the horizontal components appear to be the most appropriate.

The shapes of the APB diagrams for $P$ and $S$ waves have a very similar character for all the events. However, for $S$ waves the maxima of the curves are shifted towards longer periods. It was experienced that for events having magnitudes $m_b < 5.0$ the APB diagrams for both $P$ and $S$ waves can be constructed only in exceptional cases, the noise background, especially long-period microseisms, being the limiting factor.

For both the Tadzhik-Sinkiang and North-eastern China sequences the maxima of the APB curves vary within the period range of filters III to IX, i.e., the largest value of $A_{vmax}$ occurs in the intermediate period band. Furthermore, the general shape of the APB diagrams is practically the same for both regions without any exception.

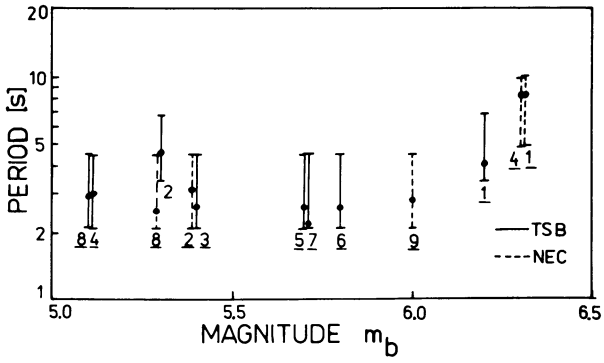


**Fig. 6.** Dependence of the passband corresponding to the largest $A_{vmax}$ value on $m_b$ magnitude for the vertical component of $P$ waves. The periods $T_v$ corresponding to $A_{vmax}$ (*solid circles*) and the numbers of the TSB and NEC events are indicated

**Table 3.** Short and medium period HMS magnitudes for the vertical component of $P$ waves

| Event | $M_{PVs}$ | $M_{PV}$ | Event | $M_{PVs}$ | $M_{PV}$ |
|---|---|---|---|---|---|
| TSB 1 | 6.85 | 6.9 | NEC 1 | 6.5 | 7.25 |
| 2 | 5.55 | 5.65 | 2 | 5.25 | 5.65 |
| 3 | 5.65 | 5.8 | 4 | 6.4 | 7.15 |
| 4 | 5.35 | 5.45 | 5 | 5.2 | – |
| 5 | 6.3 | 6.25 | 6 | 4.95 | 5.35 |
| 6 | 6.35 | 6.3 | 7 | 4.9 | – |
| 7 | 6.0 | 5.85 | 8 | 5.3 | 5.55 |
| 8 | 5.35 | 5.45 | 9 | 6.25 | 6.45 |
| 9 | 5.7 | – | | | |

The results pertaining to the vertical component of $P$ waves, mentioned in the last paragraph, are in general agreement with those obtained by Bune et al. (1973) and Zapolskij et al. (1974) on the basis of observational material from Frequency Selecting Seismic Stations. The APB diagrams for the vertical component of $P$ waves are also similar to the majority of diagrams constructed in the same way for a sequence of aftershocks from the Hokkaido region (Roglinov et al. 1978). In spite of the fact that the shapes of the APB diagrams for some of the Hokkaido events were found to be exceptionally quite different, it seems that the type of diagrams observed in the present study represents the process of seismic wave generation that prevails for shallow earthquakes.

An interesting phenomenon is the shift of the maxima of the APB diagrams towards longer periods with increasing magnitude of the events (see Figs. 3 and 4). Figure 6 shows the dependence of the passband, in which the largest $A_{vmax}$ of the vertical component of $P$ waves is found, on the magnitude $m_b$. It appears that the maxima of $A_{vmax}$ shift towards longer periods for magnitudes $m_b > 6.0$ whereas for $m_b < 6.0$ the occurrence of the largest $A_{vmax}$ in the passband from 2.2 to 4.5 s is independent of magnitude and region. The shift to filter IV for TSB event No. 2 is an exception the probable cause of which was constructive signal-noise interference. The same tendency of shifting of maxima of the APB diagrams to longer periods for events with larger magnitudes can be observed also for $S$ waves but the phenomenon is not so expressive as for $P$ waves due to the flatness of the maxima.

Using calibrating functions of the Eurasian homogeneous magnitude system HMS (Vaněk et al. 1978; Christoskov et al. 1978) the magnitudes $M_{PVs}$ and $M_{PV}$ for all the events were re-estimated on the basis of short-period and medium-period observations of the vertical component of $P$ waves. The short-period observations are approximately simulated by $A_{vmax}$ in the output of filter I and the medium-period observations by $A_{vmax}$ from those filters for which the maxima of the APB diagrams are observed. The HMS magnitudes, rounded to 0.05, are given in Table 3 without applying the station correction of KHC. It can be seen that for TSB events the agreement between $M_{PVs}$ and $M_{PV}$ is fairly good, the maximum differences being smaller than 0.15. On the contrary, for NEC events the differences between $M_{PVs}$ and $M_{PV}$ are up to 0.75 of the magnitude unit. These discrepancies can be explained by the more intense decrease of $A_{vmax}$ values in the short-period range from the maxima of the APB curves for NEC events (see Fig. 3). The differences between magnitudes $m_b$ and the HMS magnitudes $M_{PVs}$, $M_{PV}$ are caused by the different magnitude level for the Eurasian HMS in comparison with the ISC system of magnitudes (for details see Vaněk et al. 1978; Christoskov et al. 1978).

The study of times of occurrence $\tau$ of maximum velocity amplitudes reveals that in the short-period and intermediate-period range up to the band from 11.5 to 23 s the quantitiy $\tau$ usually is below 30 s for both $P$ and $S$ waves. This observation supports the recommendation accepted by the IASPEI Commission on Seismological Practice (1973) at the XVth General Assembly of the I.U.G.G. in Moscow. According to this recommendation measurements of $(A/T)_{max}$ for the determination of body wave magnitudes should be carried out in the range of 25 s from the wave onset. However, for the long-period range an increase of $\tau$ up to 70–80 s may be considered.

## Conclusions

From the study of amplitude-periodband diagrams of $P$ and $S$ waves obtained on the basis of filtered broadband records for two sequences of shallow earthquakes from the Tadzhik-Sinkiang border and from North-eastern China the following conclusions can be inferred.

The general shape of the APB diagrams for the $Z$, $NS$, and $EW$ components of $P$ and $S$ waves is similar for both regions. The diagrams are characterized by a pronounced maximum in the range of intermediate periods. The largest maximum velocity amplitudes for the regions investigated are observed in the period bands from 2.2 to 10 s for $P$ waves and from 3.4 to 23 s for $S$ waves. Because earthquake magnitude estimations are based on the principle of the largest amplitude of the wave group, observations in these period-passbands should be used for magnitude determinations from $P$ and $S$ waves. Exceptions constitute earthquakes with an anomalous behaviour of APB diagrams (e.g., Roglinov et al. 1978). This conclusion applies for shallow events in a limited magnitude range ($5.0 < m_b < 6.5$) and its general validity must be verified by further investigations.

A shift of the maximum of APB diagrams towards longer periods, observed for earthquakes with $m_b > 6.0$, and its independence on magnitude for $m_b < 6.0$, seem to be related with the process of wave generation in the focal region.

It is observed that the time of occurrence $\tau$ of maximum velocity amplitudes usually is shorter than 30 s for the short-period and intermediate-period band, and up to 80 s for the long-period band.

*Acknowledgements*. The authors wish to express their thanks to J. Horálek for processing the observational material for this study on the FBV Data Processing System. One of the authors (M.V.D.S.) thanks the Czechoslovak Academy of Sciences for providing the necessary facilities in the Geophysical Institute at Prague in order to carry out the present study under the scientific exchange programme between the Czechoslovak Academy of Sciences and the Council of Scientific and Industrial Research of India.

## References

Aranovich, Z.I., Korchagina, O.A., Horálek, J., Plešinger, A.: On the influence of seismograph responses on the estimation of earthquake magnitudes (in Russian). Travaux Inst. Géophys. Acad. Tchécosl. Sci. No. 486. Geofys. Sb. 1977 (in press)

Bune, V.I., Vvedenskaja, N.A., Gorbunova, I.V., Zapolskij, K.K., Kondorskaja, N.V., Fedorova, I.V.: To the problem of earthquake magnitude determination. Pure Appl. Geophys. **103**, 350–361, 1973

Christoskov, L., Kondorskaja, N.V., Vaněk, J.: Homogeneous magnitude system of the Eurasian continent. Tectonophysics, **49**, 131–138, 1978

Korchagina, O.A., Moskvina, A.G.: Comparative study of input signal distortions in standard class seismographs (in Russian). Izv. AN SSSR, Fiz. Zem. No. 8, 75–85, 1972

Plešinger, A., Horálek, J.: The seismic broadband recording and data processing system FBV/DPS and its seismological applications. J. Geophys. **42**, 201–217, 1976

Recommendations on Magnitude Determination in Practice of Seismic Observations by the IASPEI Commission on Seismological Practice, XV General Assembly of IUGG. Pure Appl. Geophys. **103**, 433–434, 1973

Roglinov, A., Horálek, J., Plešinger, A., Vaněk, J.: Magnitude scale structure from filtered broadband *P* wave records. Pure Appl. Geophys. **117**, 816–826, 1978

Vaněk, J., Kondorskaja, N.V., Christoskov, L.: Earthquake Magnitude in Seismological Practice, vol. 1, PV and PVs Waves (in Russian with extensive English summary). Sofia: 1978 Publ. House Bulgarian Acad. Sci. (in press)

Zapolskij, K.K., Nersesov, I.L., Rautian, T.G., Khalturin, V.I.: Physical principles of earthquake magnitude classification (in Russian). In: Magnituda i energetičeskaja klassifikacija zemletrjasenij, 79–131, Moskva 1974

Received December 12, 1977; Revised Version June 5, 1979